On the edge – taking a close look at the differentiation between tumor and stroma in digital image analysis

C. Lohse[1], P. Layer[1], N. Winkler[1], N. Fändrich-Dursun[1], D. Biljes[1], M. Khenkhar[1], K. A. David[1], H. Juhl[1], B. Gromoll[1]

[1] Indivumed GmbH, Hamburg, Germany
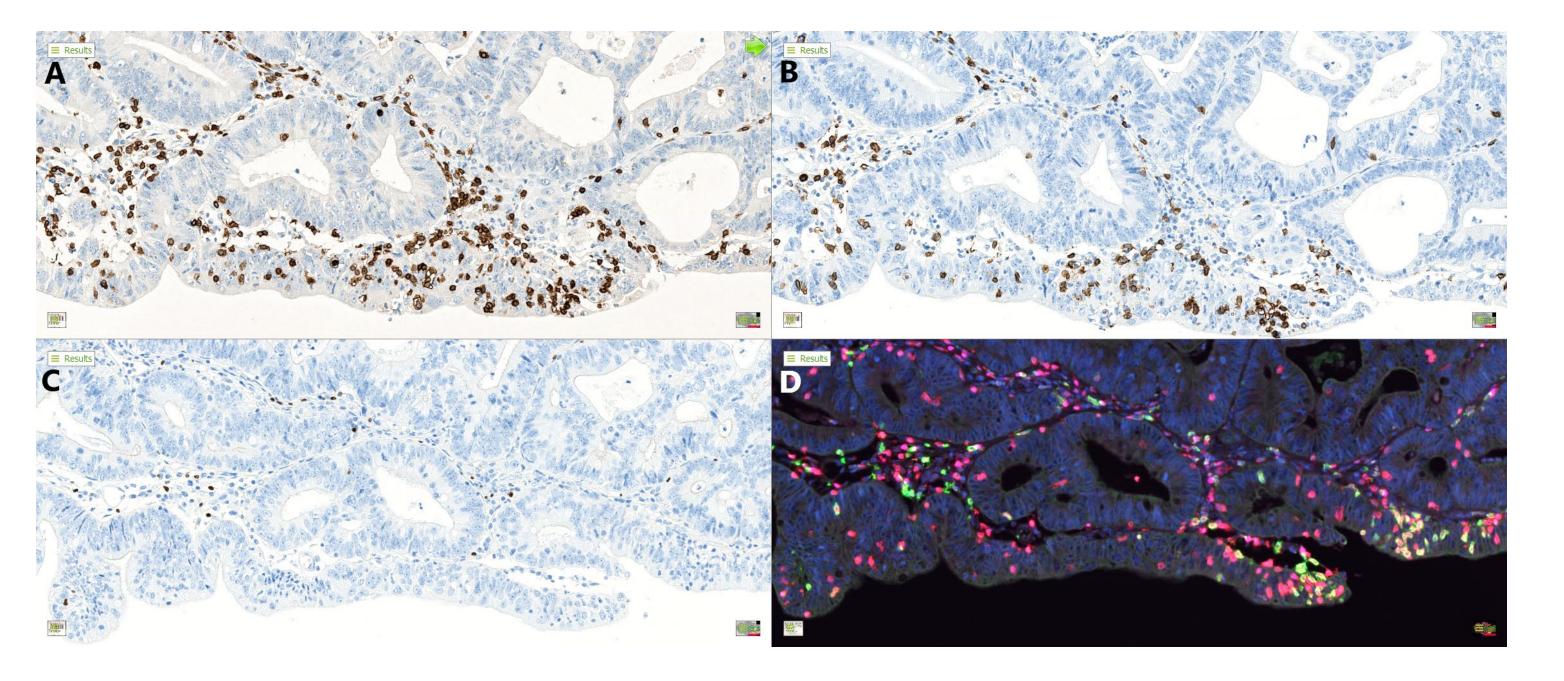
indivumed

Introduction

In digital image analysis, several algorithms are applied in a row to perform a complete analysis. With any change of method, validation tests and cross-reaction studies must be carried out to prove data integrity. Within the validation of a 5-color anti-CD3/CD8/FOXP3/pan-Cytokeratin/DAPI multiplex IHC panel with associated digital image analysis for the detection of immune cells in colorectal cancer (CRC) patient samples [1], algorithms based on chromogenic IHC and pathologist's evaluation were developed. As cell quantification showed valid results, the automated separation of tissue into tumor cells (intraepithelial compartment of cancer, short: tumor) and cells belonging to the intratumoral stroma (short: stroma), and its downstream impact on the overall analysis was examined in this poster. This was conducted regarding the determined areas of tumor and stroma, cell quantification in the determined areas and in total, as well as histopathological accuracy, as pathologists take further characteristics into account such as localization and cytomorphology.

Methods

Forty-nine FPPE CRC patient samples were stained with the above-mentioned mIHC panel and images acquired with Axio Scan.Z1 at 20x magnification. All analyses were performed with Visiopharm Oncotopix Software, Version 2019.07 and in-house developed analysis protocol packages (APP). A cell detection and quantification APP for fluorescent images was developed with pathologist's evaluation of chromogenic staining as a benchmark (Fig. 1). After the pathologist's annotation of feasible tissue area and automated tissue detection, three different analytical sequences were conducted (Fig. 2).

Figure 1: **A**: Chromogenic anti-CD3 IHC; **B**: Chromogenic anti-CD8 IHC; **C**: Chromogenic anti-FOXP3 IHC; **D**: Fluorescent anti-CD3/CD8/FOXP3/panCK/DAPI mIHC showing only CD3, CD8, FOXP3 and DAPI channels. All staining on CRC patient tissue samples.

The cell counts and whole tissue areas acquired with analytical sequence I served as reference. Differentiation between tumor and stroma areas was performed with two different algorithms: pan-Cytokeratin (panCK)/Opal570 as the only input feature in analytical sequence II and panCK/Opal570 and DAPI as input features in analytical sequence III. The two different APPs were designed to compare the reflection of the histopathological classification of cells near the tumor site. The histopathological quality of this classification was evaluated by our in-house pathologist and compared with corresponding annotations.

Figure 2: Schematic representation of three analytical sequences; I: Tissue detection APP and cell detection APP; II: APPs with inserted tumor-stroma differentiation using panCK input band only; III: APPs with inserted tumor-stroma differentiation using panCK and DAPI input bands.

Table 1: Summed results of areas, cell counts and densities in tumor areas, stromal areas and total areas for all 49 images.

	Tumor area			Stromal area			Total area		
	Area [mm²]	Cell count	Density [mm⁻²]	Area [mm²]	Cell count	Density [mm⁻²]	Area [mm²]	Cell count	Density [mm⁻²]
I	-	-	-	-	-	-	1419.12	1211041	853
II	580.29	265959	458	838.83	1027105	1224	1419.11	1293064	911
III	726.65	390093	536	688.84	852002	1236	1415.49	1242095	877

Results

The results from all three analytical sequences are shown in Table 1. Total cell counts in all 49 samples added up to $N(I) = 1.21 \times 10^6$ cells in analytical sequence I, $N(II) = 1.29 \times 10^6$ cells in analytical sequence II (percentual deviation to I: +6%) and $N(III) = 1.24 \times 10^6$ cells in analytical sequence III (percentual deviation to I: +2%). The percentual deviation in cell numbers for each sample is shown in Figure 3. Pearson correlations with analytical sequence I were calculated to $r(II) = 0.998$ for analytical sequence II and $r(III) = 0.999$ for analytical sequence III. Figure 4 shows an exemplary region with DAPI and panCK/Opal570 input bands visible. The green line in Figure 4A depicts the separation between tumor and stromal area by the pathologist's annotation, 4B shows the separation after analytical sequence II and 4C shows the separation after analytical sequence III.
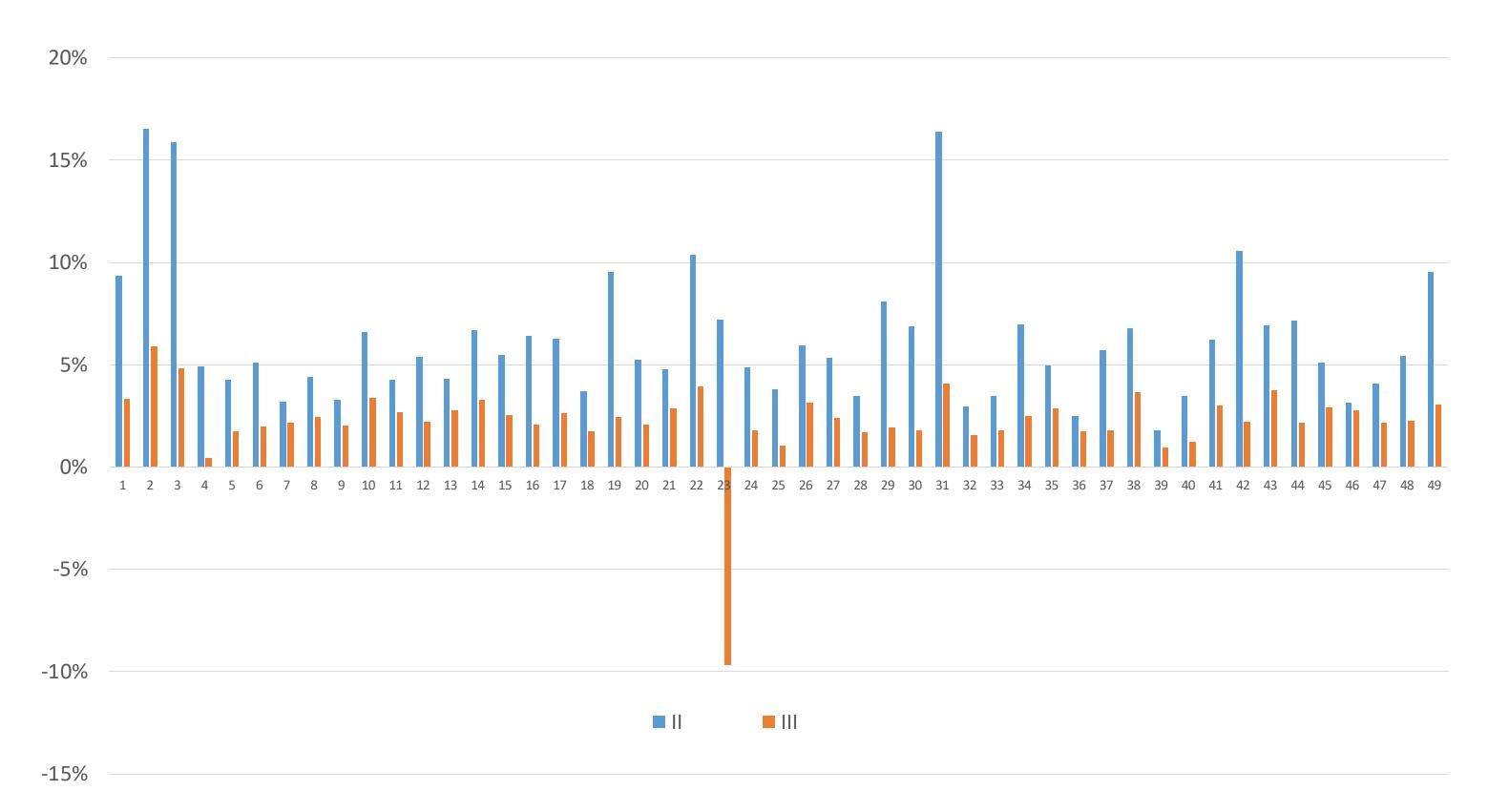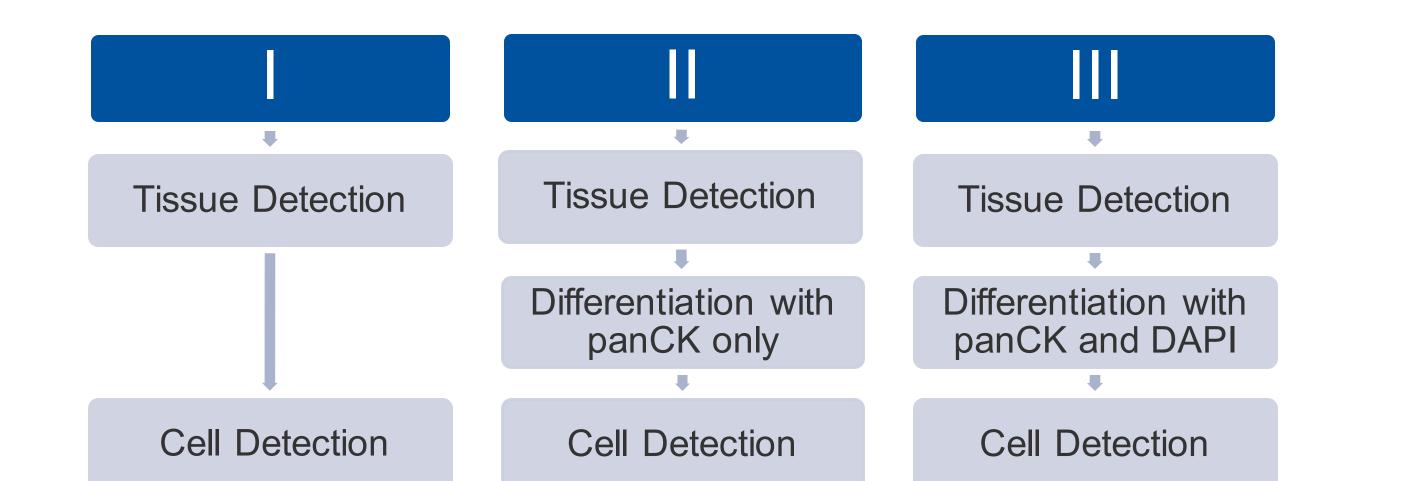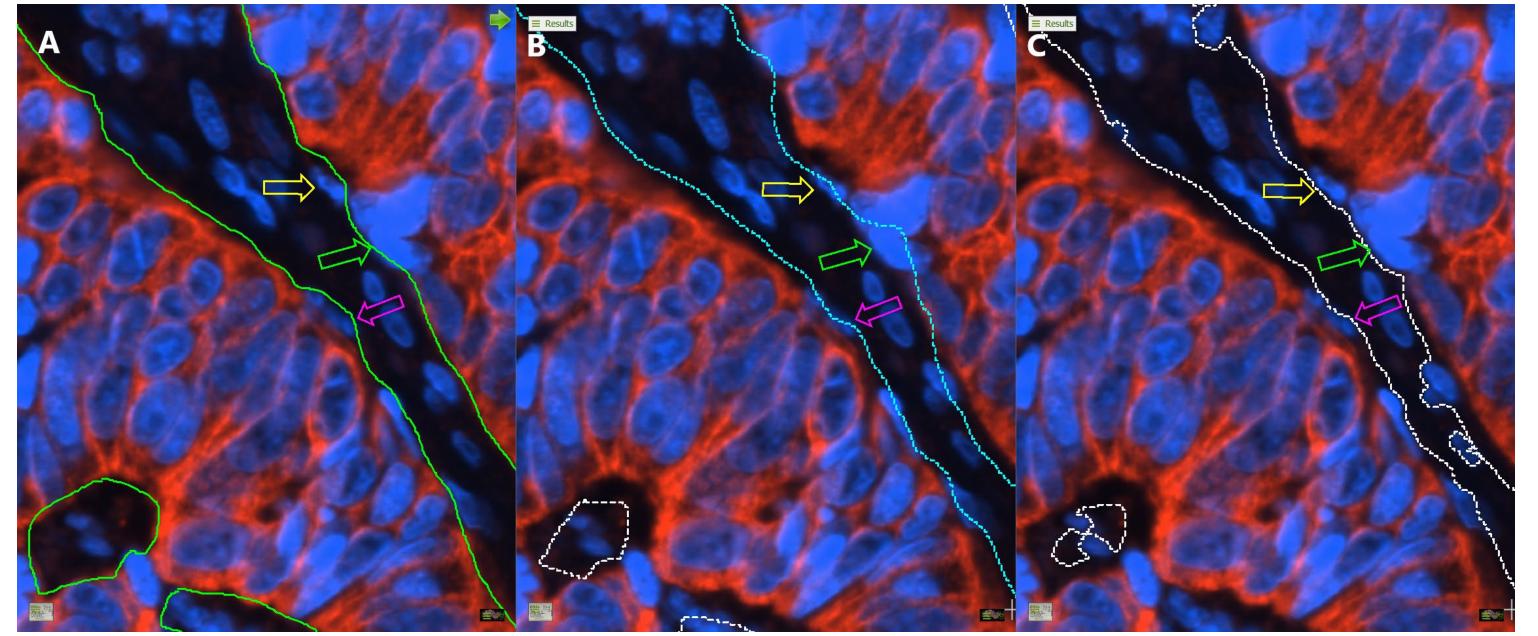

Figure 3: Percentual deviations of whole tissue cell counts from analytical sequences II (blue) and III (orange) compared to whole tissue cell counts of analytical sequence I for each of the 49 images.

Discussion

The cell count numbers increased in both analytical sequence II and III, with a median percentual deviation of +6% in analytical sequence II and +2% in analytical sequence III. The percentual deviation for each case varied in a range of 17% in analytical sequence II and 16% in analytical sequence III. Figure 3 shows that a systemic error can be excluded because the percentual deviation varied from case to case. The growth in cell numbers resulted most probably from split DAPI signals which were subsequently detected and counted more than once, as depicted by the pink and yellow arrows in Figure 4.

Improving the histopathological classification of cells near the tumor site was attempted by including DAPI as input feature into the separation between tumor and stroma, as done in analytical sequence III. This resulted in an extended outline of the tumor area throughout the tissue as seen in the increases of tumor area in Table 1 and in Figure 4C (green and yellow arrows). Compared to the pathologist's annotation, the cell marked with the yellow arrow was wrongly classified within the tumor area in analytical sequence III. In analytical sequence II, this cell was split, probably counted for tumor and stromal area and in that way increasing the total cell count.

Figure 4: mIHC images with DAPI channel in blue and panCK/Opal570 channel in orange. **A**: Pathologist's annotation, **B**: Analytical sequence II, **C**: Analytical sequence III to separate tumor and stromal area. Three arrows point at DAPI signals that are affected by the different classifications.

Conclusion

After intensive comparison and evaluation of the results, we consider analytical sequence III to be better than sequence II as it showed a lower percentual deviation in cell quantification. It should be mentioned that this only became clear in comparison with analytical sequence I, since the differences are hardly traceable through visual assessment, especially with growing data sets and high-throughput analyses. Even with a false-positive assignment of DAPI signals to the tumor area, we consider the accuracy of cell quantification after tumor-stroma-separation a success, especially since the applied algorithms are based only on threshold values and do not rely on any kind of artificial intelligence.

References:
[1] D. Biljes, P. Layer, N. Winkler, N. Fändrich-Dursun, H. Juhl, B. Gromoll, M. Khenkhar, P. Uhlig.
https://doi.org/10.1158/1538-7445.AM2019-4572